PERGAMON

International Journal of Heat and Mass Transfer 43 (2000) 4031–4042

International Journal of HEAT and MASS TRANSFER

www.elsevier.com/locate/ijhmt

Turbulent film condensation of high pressure steam in a vertical tube

Sang Jae Kim, Hee Cheon No*

Department of Nuclear Engineering, Korea Advanced Institute of Science and Technology, 371-1 Ku-song Dong, Yu-song Gu, Taejon 305-701, South Korea

Received 16 July 1999; received in revised form 29 December 1999

Abstract

An experimental study is performed to investigate the high pressure steam condensation heat transfer in a large diameter condenser tube which is adapted for passive systems in Advanced Nuclear Power Plants. Experiments are conducted with high pressure steam in a single vertical tube with an inner diameter of 46 mm at a maximum pressure of 7.5 MPa. The film condensation heat transfer coefficients in the vertical tube are calculated by the difference of measured tube wall temperatures, and the two-phase pressure drops in the condenser tube are also measured. A new turbulent annular film condensation model is developed on the basis of the similarity of pipe flow and annular film flow. The present model gives better results than those of the Shah model in comparison with the experimental data.

1. Introduction

Passive reactors such as Korea Next Generation Reactor (KNGR), Simplified Boiling Water Reactor (SBWR) are characterized by their simple design and the presence of passive systems [1]. The film condensation heat transfer in a vertical tube is key phenomena in those systems.

For the investigation of the film condensation heat transfer, a large number of experiments have been performed in vertical geometries with various fluids. Badger [2] and Shea [3] obtained the average film condensation heat transfer coefficients in vertical condensers. Carpenter [4] and Goodykoontz [5] performed the condensation experiments in vertical tubes with high steam flow rate for the measurement of the local condensation heat transfer coefficients. Blangetti [6] also reported the local condensation heat transfer coefficient in a vertical tube based on the experiment. Recently, the experiments for the investigation of the turbulence effect of liquid film in the film condensation heat transfer were carried out by Kuhn [7] and Park [8] in a tube and a rectangular channel, respectively, and the local film condensation heat transfer coefficients in highly turbulent liquid film were obtained. Peterson [9] developed models for laminar and turbulent film condensation heat transfer in vertical tubes and also proposed a transition criteria from laminar to turbulent. Vierow [10], Siddique [11], Kuhn [7], Hassanein [12] and Park [13] performed the condensation experiments in the presence of non-

* Corresponding author. Tel.: +82-42-869-3817; fax: +82-42-869-3810.

E-mail address: hcno@nesun1.kaist.ac.kr (H.C. No).

0017-9310/00/$ - see front matter
PII: S0017-9310(00)00015-6

Nomenclature

A	flow area (m^2)
a, b, c, d	constant factors in Eq. (1)
a_2, b_2, c_2	constant factors in Eq. (26)
e_1, e_2	constant factors in Eq. (31)
C_p	specific heat (J/kg K)
D	diameter (m)
F	F-factor
G	mass flux (kg/m^2)
h	heat transfer coefficient (W/m^2 K)
h_{sf}	single phase convective heat transfer coefficient (W/m^2 K)
h_f	Shah condensation heat transfer coefficient (W/m^2 K)
i_{fg}	latent heat of vaporization (J/kg)
j	superficial velocity (m/s)
k	thermal conductivity (W/m K)
l_n	vertical length of local node (m)
$\dot{m}_{cond,\ n}$	condensation rate in local node (kg/s)
$\dot{m}_f$	liquid film mass flow-rate (kg/s)
$\dot{m}_{tot}$	total mass flow rate $(\dot{m}_g + \dot{m}_f)$ (kg/s)
Nu	Nusselt number $(=\frac{h}{k_f}(\frac{\nu_f^2}{g})^{1/3})$
P	pressure (MPa)
P_{red}	reduced pressure $(= P/P_{crit})$
Pr	Prandtl number
$\dot{q}''$	heat flux (W/m^2)
r	radius of tube $[(r_{in} + r_{out})/2]$ (m)
$r_{in(out)}$	inner (outer) radius of tube (m)
Re	Reynolds number
Re_f	liquid film Reynolds number $(= \frac{4\Gamma}{\mu} = \frac{4\dot{m}_f}{\pi D\mu})$
RMS error	root mean square error, $\sqrt{\frac{(h_{correlation} - h_{experiment})^2}{h^2_{experiment}}}$
t	thickness of tube wall (m)
$t*$	corrected thickness of tube wall (m)
T_b	temperature of bulk steam (°C or K)
T_w	temperature of tube wall (°C or K)
v	velocity (m/s)
x	flow quality $(\dot{m}_g/(\dot{m}_g + \dot{m}_f))$
X_{tt}	Martinelli parameter

Greek symbols

α	void fraction
α_f	liquid fraction
Γ	mass flow-rate per unit width (kg/ms)
μ	viscosity (Pa/s)
ν	kinematic viscosity
ρ	density (kg/m^3)
σ	error of each variable
τ_i	interfacial shear stress
τ_i^*	nondimensional interfacial shear stress $(\tau_i^* = \tau_i/(\rho_f(g\nu_f)^{2/3})$
r	radius of tube (m)
r_{in}	inner radius of tube (m)
r_{out}	outer radius of tube (m)
ΔT_m	temperature difference between inner and outer wall (K)

Subscripts

h	equivalent diameter, hydraulic diameter
f	film or water phase
g	vapor or gas phase
l	liquid film phase
m	measured value
n	local position (node) of tube
in	inner wall
out	outer wall
bulk	bulk steam

condensable gases in vertical tubes. As the previous experiments have been done in relatively small diameter tubes or a rectangular channel at low pressure, there is a lack of high pressure steam condensation data for the larger diameter condenser tube, which is adapted for the passive heat removal systems in KNGR and SBWR. For the verification of those systems, it is necessary to acquire the condensation heat transfer data for the large diameter condenser tube at the high pressure conditions.

Many condensation models have been proposed for the various conditions which include the laminar and turbulent film condensation in vertical and horizontal geometries. Those models are divided into two types, a flat plate condensation model [8,14–17] and an annular film condensation model [18,19]. From the review of previous works, it is known that the governing factors of film condensation heat transfer are the velocities of liquid film and steam, and the properties of liquid film. Therefore, most of the condensation models are given by the nondimensional parameters such as Nusselt number, film Reynolds number, Prandtl number and nondimensional shear stress. Therefore, the flat plate condensation model is developed for the analysis of

the film condensation heat transfer in an inclined flat plate using those parameters as follows [17]:

$$Nu = aRe^{b}\ Pr^{c}\tau_{i}^{*d}. \tag{1}$$

A lot of wall film condensation models have been proposed following the model of Nusselt [14]. The annular film condensation models are developed for the condensation inside the condenser channel. The Shah [19] correlation, which is an empirical correlation based on a wide range of experimental data, is considered as a best correlation for the turbulent film condensation heat transfer [20]. The Shah correlation is described as follows:

$$h_{f} = h_{sf}\left(1 + \frac{3.8}{Z^{0.95}}\right), \tag{2}$$

where

$$Z = \left(\frac{1}{x} - 1\right)^{0.8} P_{red}^{0.4}. \tag{3}$$

The superficial heat transfer coefficient, h_{sf}, including the Dittus–Boelter's single phase convection heat transfer coefficient, h_{l}, is given as follows:

$$h_{sf} = h_{l}(1 - x)^{0.8}, \tag{4}$$

where

$$h_{l} = 0.023\left(\frac{k_{l}}{D}\right)Re_{l}^{0.8}Pr_{l}^{0.4}. \tag{5}$$

As the Shah correlation is considered as the most predictive condensation model for the annular film condensation model in a tube, it is used for the comparison with a correlation from the present work.

2. Experimental study

2.1. Test facility

To investigate the film condensation heat transfer in the condenser tube submerged in a water pool, a small scale experimental facility was set up and experiments have been performed to acquire the local heat fluxes,

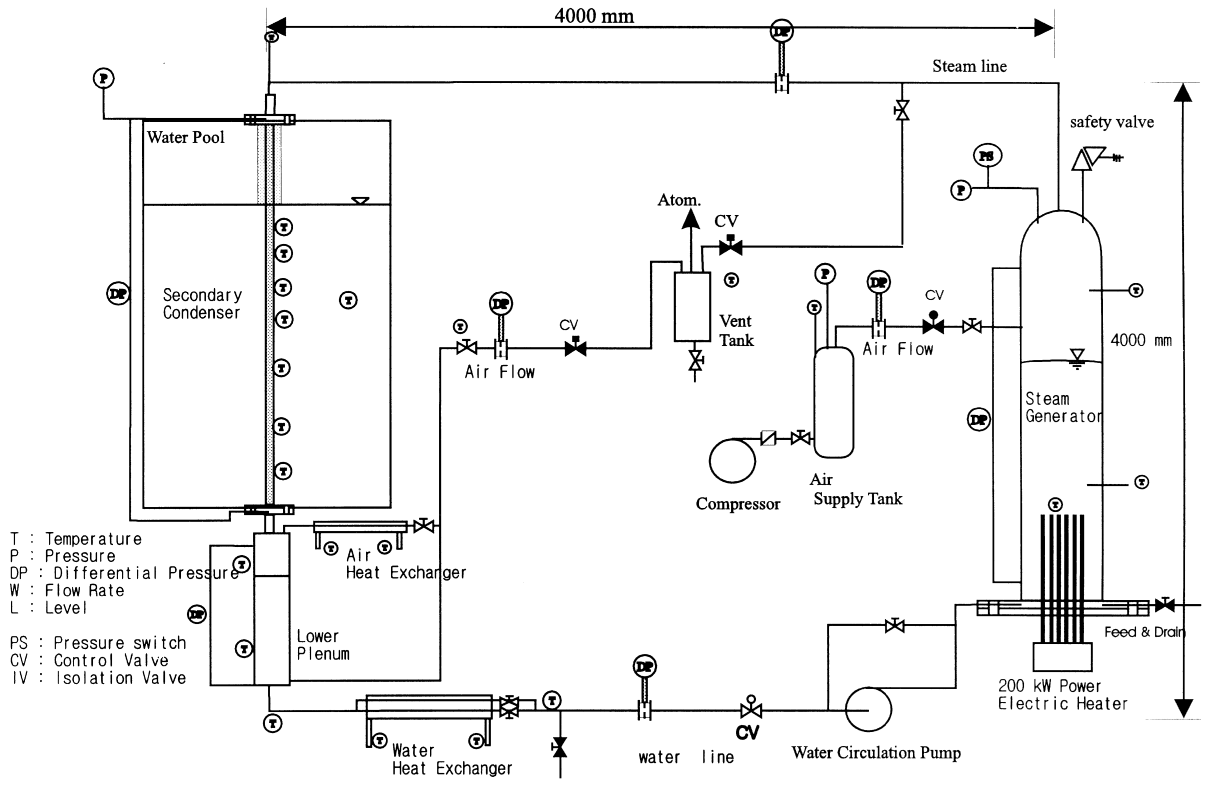

Fig. 1. Schematic diagram of test facility.

heat transfer coefficients and pressure drops in the condensation heat transfer as shown in Fig. 1. The experimental facility is designed with a maximum pressure of 7.5 MPa and a maximum temperature of 300°C. The steam generator is a 2.5 m long, 0.4 m I.D. stainless 304 tank. Its heating capacity is 200 kWe to supply steam for the condensation test at the maximum pressure of 7.5 MPa. For the experiment of condensation with noncondensable gas, the air supply system with maximum pressure of 8.0 MPa and the venting line are also included. The test section is a stainless 316 tube with an outer diameter of 50.8 mm, a thickness of 2.3 mm and a length of 1.8 m. A total of 23 K-type thermocouples with a diameter of 1 mm were silver soldered in the tube as shown in Fig. 2. As shown in section A–A in Fig. 2, sheathed ungrounded type thermocouples were installed at the center of tube to measure bulk steam temperatures at four points along the tube. Seven thermocouples are mounted at the outer surface of the tube to measure the outer wall temperatures. Sheathed grounded type thremocouples are also installed for the measurement of the inner wall temperatures at 10 points with 12 thermocouples as shown in Fig. 2. Steam line with an inner diameter of 23.4 mm is connected from the top of steam generator to the upper end of test section without valve. The steam flow rate is measured in the steam line by the orifice flow meter with the maximum error of 2.8%. The steam generated in the steam generator is directly supplied to the condenser tube. To reduce the entrance effect, a 0.5 m long, 50.8 mm O.D. tube enclosed with the teflon insulation block is installed between the top of condenser tube and the steam line.The condensate in the lower plenum is pumped to the steam generator by the water circulation pump. The test tube is submerged in a 1.2 m × 1.2 m width, 2.5 m height pool. The pool is maintained to be saturate during the experiment.

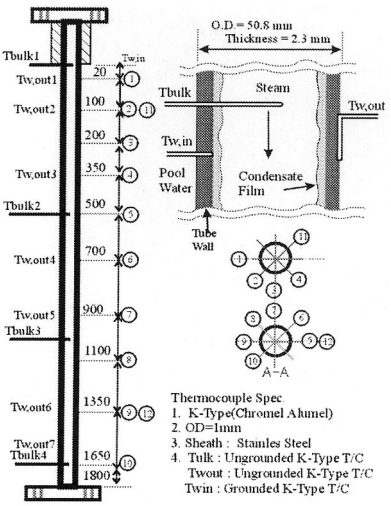

Fig. 2. Measurement of local tube wall temperatures.

2.2. Test procedure

There exist noncondensable gases in the test loop at startup. Therefore, for the removal of the noncondensable gas residing in the test loop, water in the steam generator is electrically heated and generated steam is vented to the atmosphere. The vent valve is closed after the noncondensable gas is completely removed. The steam supplied to the condenser tube is condensed and the condenser tube is gradually filled with the condensate because the water line is closed by the control valve. After the condenser tube is completely filled with the condensate, the steam generator pressure is increased to the test pressure by electric heating. After the test pressure is reached, the control valve opens and the pump starts. The constant water level in the lower plenum is maintained by controlling the pumping capacity. After the steady condition is reached, the data are acquired.

2.3. Data acquisition and reduction

To acquire the condensation heat transfer data, local temperatures and pressures are measured by the 64 channel HP-VXI DAS, which has a maximum data sampling rate of 100 kHz. The measurement system is composed of 45 thermocouples, three absolute pressure transducers and eight differential pressure transducers for the meausrements of levels and flow rates. The measured data in the DAS are transferred to the IBM PC and also used to control the test loop.

The local heat transfer coefficients and heat fluxes, which are the most important factors in the present experiment, are calculated using the temperature difference between the inner and outer condenser tube wall as shown in Fig. 2. The local heat flux is defined in terms of the temperature difference between the inner and outer wall temperatures, $\Delta T_{w,\,n}$, in the local node, n, as follows:

$$\dot{q}_n'' = k_{\text{wall},\,n}\frac{\Delta T_{w,\,n}}{r/2l_n(r_{out}/r_{in})}, \tag{6}$$

where r_{out} and r_{in} are the inner and outer radii of the test tube, respectively. The local heat transfer coefficient is given by the local heat flux and the local temperatures as follows:

$$h_n = \frac{\dot{q}_n''}{T_{\text{bulk},\,n} - T_{w,\,\text{in},\,n}} \tag{7}$$

To obtain the conductivity of the stainless-steel 316 tube, a simple correlation is developed from the linear fit of the data extracted from the property Table of Incropera [21] with the maximum error of 1.5% as follows:

$$k_{\text{wall},\,n} = 14.49 + 0.0163\left[\left(T_{\text{w, in},\,n} + T_{\text{w, out},\,n}\right)/2\right]. \quad (8)$$

The local steam condensation rate is calculated from the measured local heat flux as follows:

$$\dot{m}_{\text{cond},\,n} = \frac{\dot{q}''_n \pi D l_n - \Delta T_{\text{f},\,n} C_{\text{pf},\,n} \dot{m}_{\text{f},\,n-1}}{i_{fg,\,n} + \left(T_{\text{g},\,n} - T_{\text{f},\,n}\right) C_{\text{pf},\,n}}. \quad (9)$$

where the temperature change of liquid film, $\Delta T_{\text{f},\,n}$, is calculated from the mean film temperatures obtained from the temperatures of the bulk steam and the inner wall as suggested by McAdams [22].

$$\Delta T_{\text{f},\,n} = T_{\text{f},\,n-1} - T_{\text{f},\,n}. \quad (10)$$

where the local film temperature is calculated as follows:

$$T_{\text{f},\,n} = T_{\text{bulk},\,n} - 3/4\left(T_{\text{bulk},\,n} - T_{\text{w, in},\,n}\right). \quad (11)$$

The local film flow rate is calculated from the local steam condensation rate as follows:

$$\dot{m}_{\text{f},\,n} = \dot{m}_{\text{f},\,n-1} + \dot{m}_{\text{and},\,n}. \quad (12)$$

Finally, the flow quality, x_n, is calculated from the local mass flow rates as follows:

$$x_n = \frac{\dot{m}_{\text{g},\,n}}{\dot{m}_{\text{f},\,n} + \dot{m}_{\text{g},\,n}} = \frac{\dot{m}_{\text{tot}} - \dot{m}_{\text{f},\,n}}{\dot{m}_{\text{tot}}}. \quad (13)$$

where the total mass flow rate supplied to the condenser tube, $\dot{m}_{\text{tot}}$, is sum of the local steam flow rate and the local film flow rate.

2.4. Data correction and uncertainty analysis

The present heat flux measurement method mentioned above is not usually adopted because of the large measurement uncertainties of the inner and outer wall temperatures. In several condensation experiments, the cooling jacket is introduced for the measurement of the local heat transfer coefficients in a tube [7]. The objective of the present experiment includes both the condensation heat transfer coefficient and the pool boiling heat transfer coefficient measurement in a condenser tube submerged in a pool. Therefore, the direct wall temperature measurement method is selected instead of the cooling jacket method.

For the verification and correction of the measured tube wall temperatures, the correction experiments has been performed. The correction experiment is a single phase turbulent convection heat transfer test in the condenser tube as shown in Fig. 3. High temperature water of 250°C is supplied from the bottom of condenser tube at the pressure of 4.5 MPa whereas the water in the pool is subcooled at atmospheric pressure. The bulk temperature of supplied water in the center of tube shows gradually decreasing trend from the bottom of the tube due to the heat transfer through the tube wall. The conductive heat flux through the tube wall becomes same as the turbulent convective heat

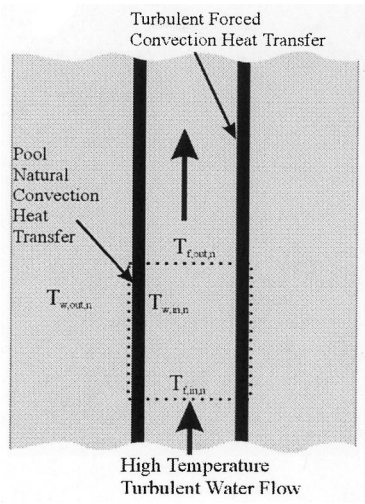

Fig. 3. Schematic of wall temperature correction experiment.

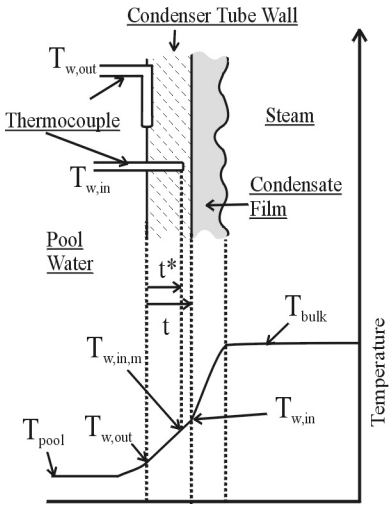

Fig. 4. Temperature profile across tube wall with thermocouples.

flux inside the tube in the control volume, shown in Fig. 3.

In the correction experiment, the local heat fluxes are directly measured from the wall attached thermocouples as given in Eq. (6) and also given by the temperature drops of the supplied water flow as follows:

$$\dot{q}''_{\text{conv},\,n} = \frac{C_{\text{p}}\dot{m}_{\text{f}}}{\pi D l_{\text{tube}}}\left(T_{\text{f, in},\,n} - T_{\text{f, out},\,n}\right). \tag{14}$$

The local inner wall temperatures are corrected from the comparison of the above two heat fluxes. For the correction of inner wall temperature, the local positions of inner wall thermocouples, t_n^*, are acquired from the comparison of $\dot{q}''_n$ and $\dot{q}''_{\text{conv},\,n}$. t_n^* means the depth of installed thermocouple for inner wall temperature as shown in Fig. 4. Using t_n^*, the true value of inner wall temperature is calculated as follows:

$$T_{\text{w, in},\,n} = \frac{t_n^*}{t}T_{\text{w, in, m},\,n} + \left(1 - \frac{t_n^*}{t}\right)T_{\text{w, out},\,n}. \tag{15}$$

where $T_{\text{w, in, m},\,n}$ means the measured local inner wall temperature.

The uncertainty analysis of the local heat transfer coefficients is performed using the error propagation method [23]. The sources of uncertainty have originated from the measurement errors of the instruments. The condensation heat transfer coefficient derived from Eqs. (6) and (7) is given as a function of local temperatures, conductivity and radii.

$$h = \frac{k_{\text{wall}}}{r/l_n(r_{\text{out}}/r_{\text{in}})}\frac{T_{\text{w, in}} - T_{\text{w, out}}}{T_{\text{bulk}} - T_{\text{w, in}}} \tag{16}$$

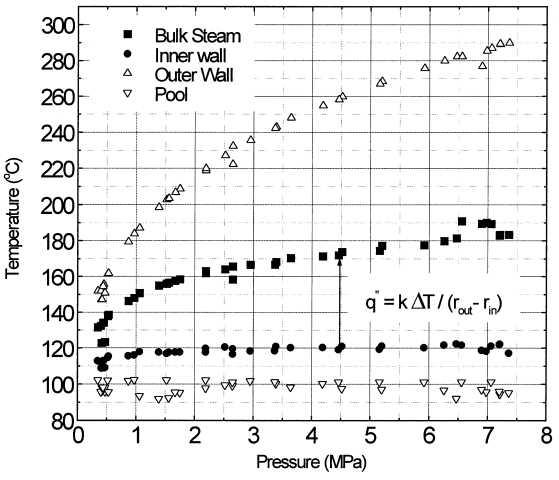

Fig. 5. Local temperatures as a function of pressure.

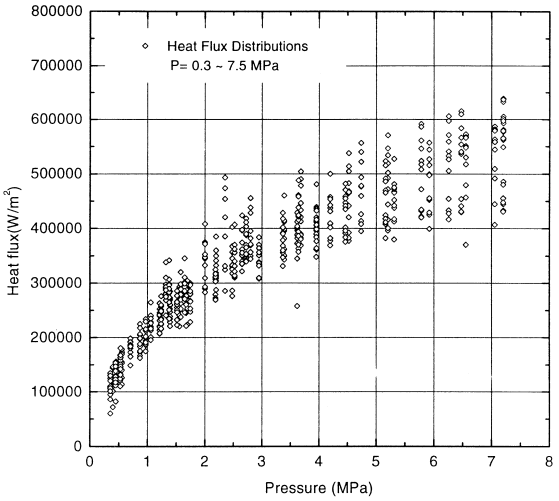

Fig. 6. Local heat fluxes as a function of pressure.

and

$$h = f\left[\, T_{\text{w, in}},\quad T_{\text{w, out}},\quad T_{\text{bulk}},\quad k_{\text{wall}},\quad r\,\right], \tag{17}$$

where the uncertainty of k_{wall} also depends on the uncertainty of tube wall temperatures because it is given as a function of wall temperatures in Eq. (8). The uncertainty of heat transfer coefficient is estimated from the instrumental errors of the measurement devices as follows:

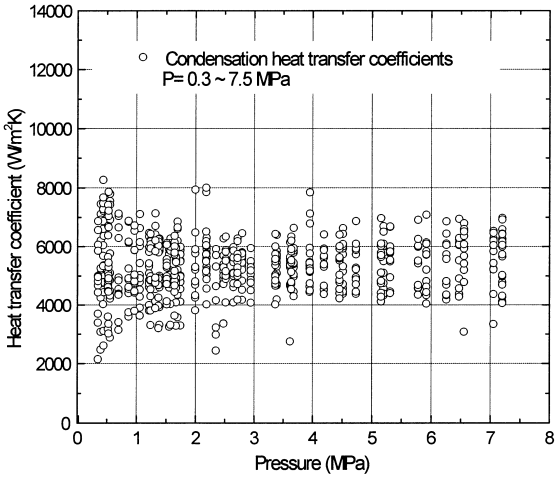

Fig. 7. Local heat transfer coefficients as a function of pressure.

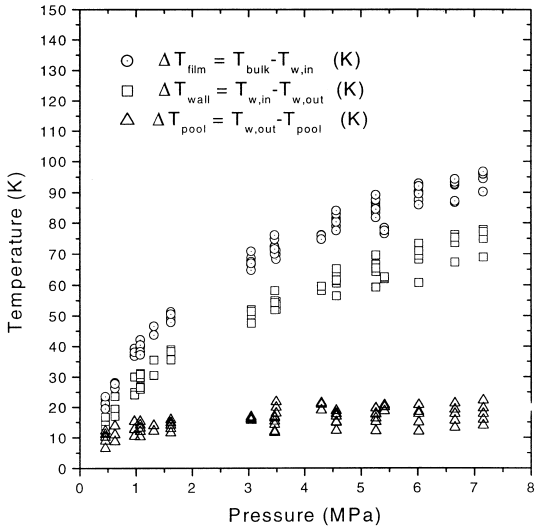

Fig. 8. Comparison of local temperature differences.

$$\sigma_h = \left[\sigma^2_{T_{\mathrm{w,\,in}}} \left(\frac{\partial h}{\partial T_{\mathrm{w,\,in}}} \right)^2 + \sigma^2_{T_{\mathrm{w,\,out}}} \left(\frac{\partial h}{\partial T_{\mathrm{w,\,out}}} \right)^2 + \sigma^2_{T_{\mathrm{bulk}}} \left(\frac{\partial h}{\partial T_{\mathrm{bulk}}} \right)^2 + \sigma^2_{k_{\mathrm{wall}}} \left(\frac{\partial h}{\partial k_{\mathrm{wall}}} \right)^2 + \sigma^2_r \left(\frac{\partial h}{\partial r} \right)^2 \right]^{1/2} \tag{18}$$

The uncertainties of inner wall temperatures, outer wall temperatures and bulk temperature are estimated as 6%, 2% and 1.5%, respectively. The error bound of radius, r, is $\pm 3\%$. The uncertainty of k_{wall} is calculated to 2.5%. Finally, the uncertainties of condensation heat transfer coefficient are obtained to 28.2% from Eq. (18). The uncertainty of condensation heat flux is also estimated as 15.9%.

2.5. Experimental results

2.5.1. Condensation heat transfer coefficient

A total of 984 local data of film condensation heat transfer including laminar and turbulent flow regimes are acquired in the range of pressure from 0.35 to 7.2 MPa.

Fig. 5 shows the measured local temperatures of bulk, inner wall, outer wall and pool as a function of pressure. The local heat fluxes and heat transfer coefficients are calculated from the temperatures of inner wall and outer wall using Eqs. (6) and (7). Figs. 6 and 7 show the local heat fluxes and the heat transfer coefficients as a function in pressure. The heat fluxes increase with an increase of pressure. However, the heat transfer coefficients lie within a range of 4000–7000 W/m^2 K regardless of the system pressure.

There exist three heat resistances of the condenser tube; the film condensation on the inner wall, the wall conduction and the pool boiling on the outer wall. The heat resistance is represented by the temperature differences between bulk, inner wall, outer wall and pool as shown in Fig. 8. The temperature differences of the condensation is largest among them. Based on the measured heat fluxes, the local condensation rates and local film mass flow rates are calculated in the tube. The laminar to turbulent transition lengths are obtained from the local film mass flow rates as shown in Fig. 9. There exist several definitions for the critical Reynolds number in the range of 576–4000 [24]. Recently, Peterson [9] proposed a transition Reynolds number correlation using Prandtl number and nondimensional interfacial shear stress based on several

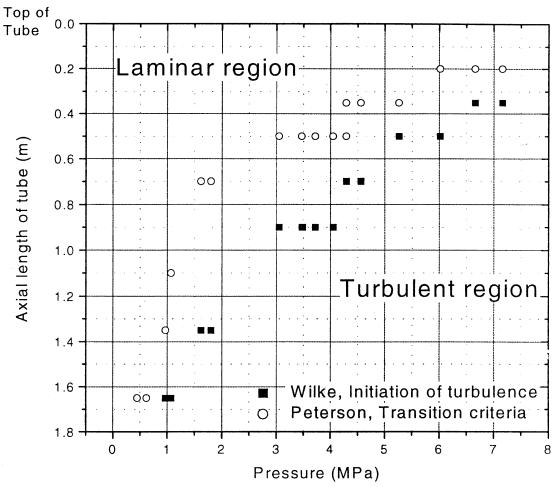

Fig. 9. Transition lengths as a function of pressure.

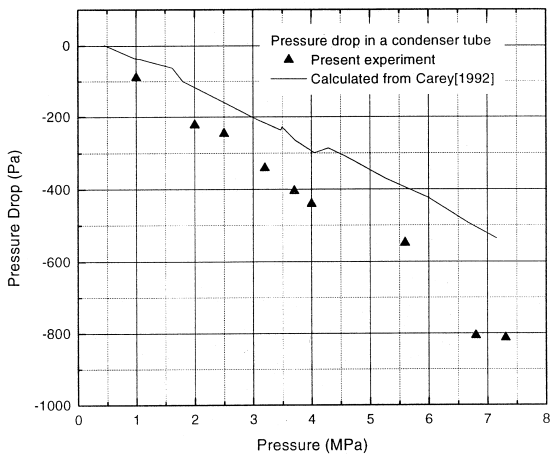

Fig. 10. Pressure drop in a condenser tube.

experimental data as follows:

$$Re_{tr} = 4080\left[\left(1 + 0.31\tau_i^{*1.07}\right)\left(1.18Pr_f^{0.87} - 0.23\right)\right]^{-1}. \tag{19}$$

Also, Wilke [25] developed a correlation for departure Reynolds number from liminar flow as follows:

$$Re_{tr} = 2460Pr^{-0.65}. \tag{20}$$

The transition Reynolds number of Peterson is adopted in the present experiment. The 107 turbulent film condensation data from the turbulent region in Fig. 9 are gathered and used for the development of condensation model in the following section.

2.5.2. Pressure drop in a vertical tube

The accurate estimation of the pressure drop in a condenser tube is also important to the condenser design. Therefore, the differential pressure (ΔP) between the tube inlet and the tube outlet is measured by the differential pressure transmitter. The two-phase pressure drop in the annular film flow is given by the sum of gravitational pressure drop, frictional pressure drop and accelerational pressure drop [26].

$$\frac{dP}{dz} = \left(\frac{dP}{dz}\right)_{gra} + \left(\frac{dP}{dz}\right)_{fr} + \left(\frac{dP}{dz}\right)_{acc},$$

$$\left(\frac{dP}{dz}\right)_{gra} = \rho_v g h_l,$$

$$\left(\frac{dP}{dz}\right)_{fr} = 0.079\left[\frac{Gx(D-\delta)}{\mu_v(1-4\delta/D)}\right]^{-0.25}\left(\frac{G^2x^2}{2\rho_v(1-4\delta/D)}\right),$$

$$\left(\frac{dP}{dz}\right)_{acc} = -\frac{2xDG^2}{\rho_v(D-2\delta)}\frac{dx}{dz}. \tag{21}$$

where h_l is the vertical length of condenser tube, δ is the film thickness and x is the quality of the two-phase annular flow.

Fig. 10 shows the comparison of the measured differential pressures with the predictions from Eq. (21). The negative value of the pressure drop means an increase of pressure along the downward axial length of tube. The two-phase frictional and accelerational pressure drops calculated from the present experimental data are very small in comparison with the gravitational pressure drop as shown in Fig. 11. The estimated error of measured differential pressure is about 5%.

3. Turbulent annular film condensation model

3.1. Development of turbulent annular film condensation model

A turbulent film condensation model in a vertical tube is developed using the similarity between the single phase turbulent convective heat transfer and the annular film condensation heat transfer as shown in Fig. 12. In the turbulent film flow regime, the governing heat transfer mechanism of annular film condensation is also turbulent convection of film.

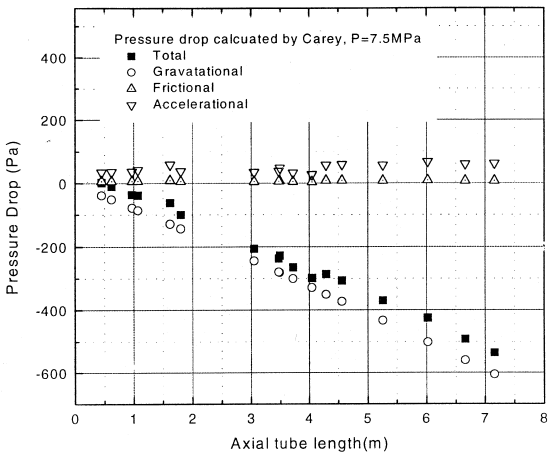

Fig. 11. Pressure drops calculated by Eq. (21).

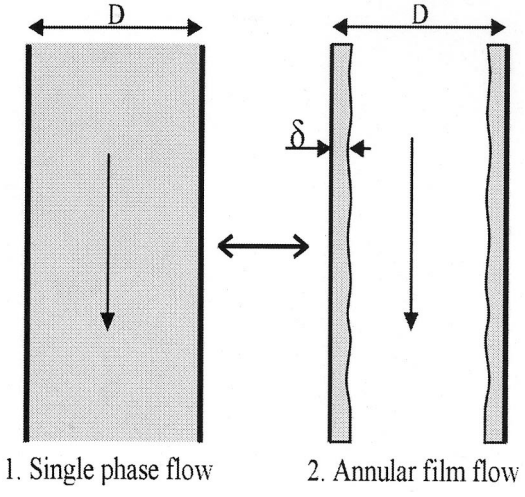

Fig. 12. Two flow patterns in a vertical tube.

Reynolds numbers of the single phase flow regime and the annular film flow regime are derived as follows:

$$Re_1 = \frac{G(1-x)D}{\mu_f} = \frac{\rho_f v_f \alpha_f D}{\mu_f}, \tag{22}$$

where $G(1-x) = G_f = \rho_f j_f$, and

$$Re_2 = \frac{\rho_f v_f D_h}{\mu_f} = \frac{\rho_f \alpha_f v_f D}{\mu_f}, \tag{23}$$

where $D_h = 4\frac{A_f}{P} = 4\delta_f(1-\delta_f/D)$, $D_h = \alpha_f D$.

It is assumed that liquid only flows in the channel of the single phase flow, the mechanism of heat transfer is convection, no nucleation occurs at the wall in the two-phase film flow, and there is no entrainment in the channel. If liquid mass flux is the same in both flow regimes 1 and 2, the ratio of Reynolds numbers becomes 1 as follows:

$$\frac{Re_1}{Re_2} = 1. \tag{24}$$

The Dittus–Boelter correlation is known as a well predicting correlation for the single phase turbulent convective pipe flow (flow regime 1):

$$h_1 = h_{\text{dittus}} = 0.023 k_f Re_1^{0.8} Pr_f^{0.4}/D. \tag{25}$$

The governing heat transfer mechanism is also turbulent convective heat transfer of falling film in the annular film flow regime. Therefore, the heat transfer coefficient in the film flow can be determined using the same nondimensional parameters:

$$h_2 = a_2 k_f Re_2^{b_2} Pr_f^{c_2}/D_h. \tag{26}$$

The ratio of the heat transfer coefficients is given with the definition of the F factor, which is equivalent to the Reynolds number factor defined by Chen [27], as follows:

$$F = \frac{h_2}{h_1} = \frac{a_2}{0.023}\frac{1}{\alpha_f}\left(\frac{Re_2}{Re_1}\right)^{(b_2-0.8)} Pr_f^{(c_2-0.4)}. \tag{27}$$

According to Chen [27], as the F factor depends on the Martinelli parameter, X_{tt}, only, b_2 and c_2 become 0.8 and 0.4, respectively. Then, it can be expressed in terms of α_f:

$$F = \frac{a_2}{\alpha_f}. \tag{28}$$

Finally, the film flow heat transfer correlation is derived from the above Eq. (28) as follows:

$$h_2 = \frac{f_D}{(1-\alpha)} Re_2^{0.8} Pr_f^{0.4} \frac{k_f}{D}, \tag{29}$$

where the factor of diameter, f_D, accounts for the effect of the diameter on film condensation, which becomes 1 for the tube diameter of 50 mm. Finally, the condensation heat flux is given by the condensation heat transfer coefficient and temperature as follows:

$$h_2 = \frac{\dot{q}''}{\Delta T} = \frac{\dot{q}''}{(T_g - T_{w,\text{in}})} \tag{30}$$

A lot of void fraction and quality correlations have been developed for various flow regimes [28]. In the present model, the void fraction of the two phase film

Table 1
Summary of compared experimental data

	Present	Goodykoontz [5]	Kuhn [7]
Type	Steam condensation	Steam condensation	Condensation on film
Geometry	Single tube	Single tube	Single tube
Tube diameter, D (mm)	46	15.8, 7.4	48.2
Tube length, L (m)	1.8	2.4	2.4
Tube material	Stainless steel	Copper	Stainless steel
Cooling	Pool	Cooling jacket	Cooling jacket
Heat transfer coefficient measurement	Wall temperature	Coolant temperature	Coolant temperature
Condensing fluid	Water	Water	Water
Reynolds number, Re_f	2400–18,000	1000–50,000	5000–29,000
Prandtl number, Pr	0.84–1.27	1.44–2.81	1.4–2.11
Pressure (MPa)	0.35–7.2	0.5	0.3
Maximum heat flux (kW/m ^{2})	708	1034	174
Maximum heat transfer coefficient (W/m^2 K)	7400	90,000	17,500
Data point	107	92	1230

flow is defined in the same form as the Lockhart–Martinelli correlation as follows:

$$\alpha = \left(1 + X_{\mathrm{tt}}^{e_1}\right)^{e_2}, \tag{31}$$

where the Martinelli parameter is

$$X_{tt} = \left(\frac{\mu_l}{\mu_v}\right)^{0.25}\left(\frac{1-x}{x}\right)^{1.75}\left(\frac{\rho_v}{\rho_l}\right). \tag{32}$$

The relation of void fraction in Eq. (31) shows large scattering near the high void fraction and low Martinelli parameter [28]. Therefore, the best fit relation of the void fraction is founded for the present experiment from the comparison of the present model with the experimental data. The factors of e_1, e_2 for the present experimental data are selected as 0.6, −0.15, respectively. Then, the diameter factor, f_D, is empirically derived from the experimental data given in Table 1 as follows:

$$f_D = 0.0182\left[1 - 0.24(1 - 4.47D^{0.5})\right]^4. \tag{33}$$

Using the diameter factor, the present model predicts well all of the turbulent film condensation data in Table 1. The present correlation is applicable for the turbulent annular film condensation in a vertical tube and the recommended range of tube diameter is from 7.4 to 50 mm.

3.2. Discussion of results

The turbulent annular film condensation models of the present and Shah are assessed with various experimental data. The data from three vertical in-tube condensation experiments are compared with the predictions from the models. Those data are summarized in Table 1. There exist little data of steam condensation inside a vertical tube. The experiment of Goodykoontz [5] and Kuhn [7], in which the local properties and the heat transfer coefficients are measured at low pressure, are selected for the comparison. The 107 turbulent film condensation heat transfer coefficient data in the present experiment are extracted

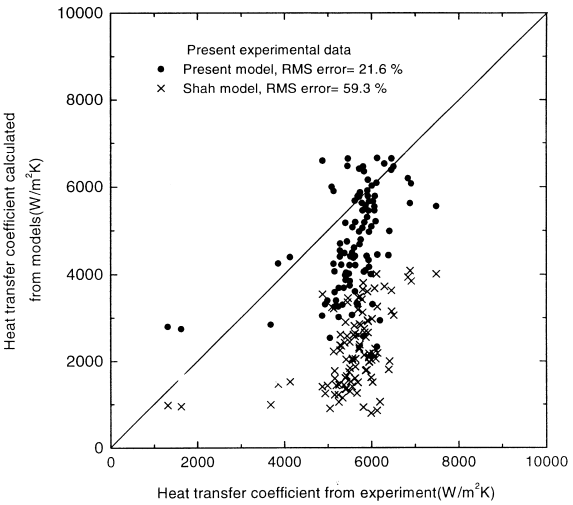

Fig. 13. Comparison of condensation models with the present experimental data.

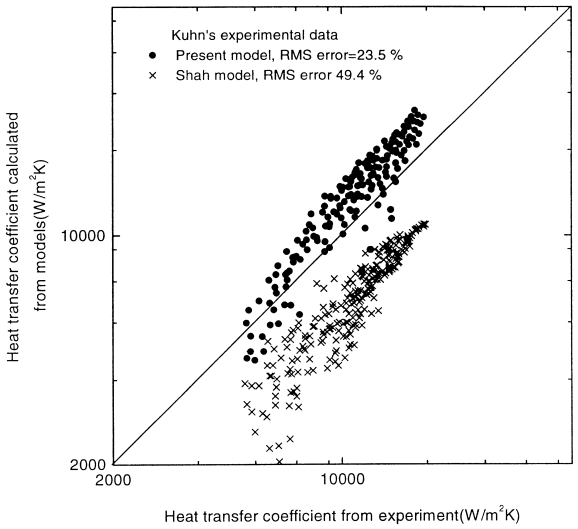

Fig. 14. Comparison of condensation models with the data of Kuhn [7].

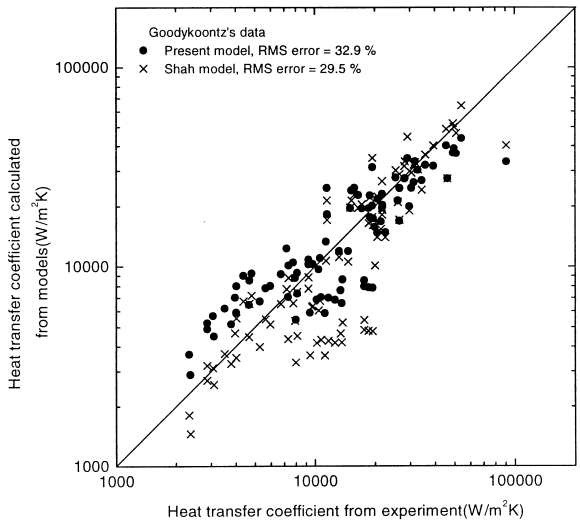

Fig. 15. Comparison of condensation models with the data of Goodykoontz [5].

for the verification of the present model. Goodykoontz obtained the heat transfer coefficients from the condensation experiment of high speed steam in relatively small diameter tubes. Kuhn performed the steam condensation experiment on the turbulent film generated by the film distributor in a relatively large diameter tube.

Figs. 13–15 show the comparison results of the experimental data with the two condensation models. As shown in Figs. 13 and 14 the Shah model underpredicts the data of the present and the Kuhn experiment [7] performed in the relatively large diameter tubes by about 50%, while the present model gives more reasonable predictions for those data. It is due to this that the Shah model, based on the condensation heat transfer data in a diameter of smaller than 40 mm, is developed and usually used for the estimation of refrigerator performance. As shown in Fig. 13, the range of heat transfer coefficient in the present experiment is very limited because the system pressure is a control variable and the film Reynolds number, which is a dominant factor in the heat transfer coefficient, slightly increases with an increase in pressure.

Both the present model and the Shah model well predict the data of Goodykoontz [5] as shown in Fig. 15.

The mean RMS errors of the present model and the Shah model with equal weight of each data are 26% and 46.1%, respectively.

4. Conclusions

The high pressure steam condensation experiments are performed in a vertical tube with an inner diameter of 46 mm to investigate the turbulent film condensation at a steam pressure of 7.5 MPa. The local condensation heat transfer coefficients and the pressure drops in the condenser tube are acquired. The turbulent film condensation heat transfer coefficients are compared with the Shah model. The Shah model does not show good agreement with the data in a relatively large diameter tube such as the present and the Kuhn ones. Therefore, a new analytical condensation model is developed based on the annular film flow model. The developed model gives better estimations for the present and the Kuhn data than the Shah model does.

Acknowledgements

The authors gratefully acknowledge financial support from the Korea Electric Power Research Institute (KEPRI).

References

[1] S.H. Chang, H.C. No, W.P. Baek, S.I. Sang, S.W. Lee, Korea looks beyond the next generation, Nuclear Engineering International 24 (1997) 553–562.
[2] W.L. Badger, C.C. Monrad, H.W. Diamond, Evaporation of caustic soda to high concentrations by means of diphenyl vapors, Industrial and Engineering Chemistry 22 (1930) 700–707.
[3] F.L. Shea, N.W. Krase, Drop-wise and film condensation of steam, Trans AIChE 36 (1940) 463–489.
[4] F.G. Carpenter, Heat transfer and pressure drop for condensing pure vapors inside vertical tubes at high vapor velocities, Ph.D. Thesis, University of Delaware, 1948.
[5] J.H. Goodykoontz, R.G. Dorsch, Local heat-transfer coefficients for condensation of steam in vertical down ow within a 5/8 inch-diameter tube, NASA TN D-3326, 1966.
[6] F. Blangetti, R. Krebs, E. Schlunder, Condensation in vertical tubes — experimental results and modelling, Chemical Engineering Fundamentals 1 (1982) 20–63.
[7] S.Z. Kuhn, Investigation of heat transfer from condensign steam–gas mixtures and turbulent films flowing downward inside a vertical tube, Ph.D. Thesis, University of California, Berkely, 1995.
[8] S.K. Park, M.H. Kim, K.J. Yoo, Condensation of pure steam and steam–air mixture with surface waves of condensate film on a vertical wall, Int. J. Multiphase flow 22 (1996) 893–908.
[9] P.F. Peterson, V.E. Schrock, S.Z. Kuhn, Recent experiments for laminar and turbulent film heat transfer in vertical tubes, Nuclear Engineering and Design 175 (1997) 157–166.
[10] K.M. Vierow, V.E. Schrock, Condensation in a natural circulation loop with noncondensable gases. Part I — heat transfer, in: Proceeding of the Int. Conf. on Multiphase Flows '91-Tsukuba, 1991, pp. 183–186.
[11] M. Siddique, M.W. Golay, M.S. Kazimi, Local heat transfer coefficients for forced-convection condensation of steam in a vertical tube in the presence of a noncondensable gas, Nuclear Technology 102 (1993) 386–402.
[12] H.A. Hassanein, M.S. Kazimi, M.W. Golay, Forced convection in-tube steam condensation in the presence of noncondensable gases, International Journal of Heat and Mass Transfer 39 (1996) 2625–2639.
[13] H.S. Park, H.C. No, A condensation experiment in the presence of noncondensables in a vertical tube of a passive containment cooling system and its assessment with RELAP5/MOD3.2, Nuclear Technology 127 (1999) 1–10.
[14] W. Nusselt, Die Ober achenkondensation des Wasserdampfes — the surface condensation of water, Zeitschrift Vereines Deutscher Ingenieure 27 (1916) 541–546.

[15] S.S. Kutateladze, Semi-empirical theory of film condensation of pure vapours, Int. J. of Heat and Mass Transfer 25 (1982) 653–660.
[16] S.J. Chen, Turbuelent film condensation on a vertical plate, in: Proceedings of Int. Heat Transfer Conf., San Franscio, vol. 4, 1986, pp. 1601–1606.
[17] K.Y. Choi, H.S. Park, S.J. Kim, H.C. No, Assessment and improvement of condensation models in RELAP5/MOD3.2, Nuclear Technology 124 (1998) 103–117.
[18] D.P. Traviss, W.M. Rohsenow, A.B. Baron, Forced-convection condensation inside tubes: a heat transfer equation for condenser design, ASHARE Trans. 79 (1973) 157–165.
[19] M.M. Shah, A general correlation for heat transfer during film condensation inside pipe, Int. J. of Heat Mass Transfer 22 (1979) 547–556.
[20] General Electric Company, Heat and Fluid Flow Data Book, Genium Publishing, 1990, p. 506.3.
[21] F.P. Incropera, D.P. Dewitt, Fundamentals of Heat and Mass Transfer, 3rd ed., Wiley, New York, 1990.
[22] W.H. McAdams, Heat transmission, 3rd ed., McGraw-Hill, New York, 1954.
[23] E.O. Doebelin, Measurement Systems — Application and Design, 4th ed., McGraw-Hill, New York, 1977, pp. 58–60.
[24] K.T. Kim, A semi-empirical heat transfer coefficient for laminar and turbulent film condensation on a vertical surface, Ph.D. Thesis, Korea Advanced Institute of Science and Technology, Korea, 1991.
[25] K.R. Chun, Heat transfer to evaporating liquid films, Journal of Heat Transfer 93 (1971) 391–396.
[26] V.P. Carey, Liquid–Vapor Phase-Change Phenomena, Hemisphere Publishing Co, Washington, DC, 1992, p. 458.
[27] J.C. Chen, A correlation for boiling heat transfer to saturated liquids in convective flow, in: ASME–AIChE Heat Transfer Conference, 1963, pp. 2–11.
[28] G.B. Wallis, One-Dimensional Two-Phase Flow, McGraw-Hill, New York, 1969, pp. 49–60.